Materials Transactions, Vol. 44, No. 4 (2003) pp. 677 to 680

Crystal Structure of Fe–N Clusters Prepared by Plasma-Gas-Condensation*[1]

Dong-Liang Peng*[2], Takehiko Hihara and Kenji Sumiyama

Department of Materials Science and Engineering, Nagoya Institute of Technology, Nagoya 466-8555, Japan

Fe–N clusters were prepared by a plasma-gas-condensation cluster deposition apparatus at various nitrogen gas flow rate R_{N_2}, and their crystal structures were investigated by transmission electron microscopy. For $R_{N_2} > 2.2 \times 10^{-7}$ mol/s, fcc single-phase FeN clusters are obtained and their lattice parameter is $a = 0.428$ nm, being close to that ($a = 0.433$ nm) of ZnS-type FeN films. When $R_{N_2} \geq 7.5 \times 10^{-7}$ mol/s, almost all clusters are of a tetrahedron shape with cluster sizes of $d = 8$–25 nm. This reveals that the tetrahedron shape of FeN compound clusters is stable in such small sizes, implying a low (111) surface energy and/or high elastic strain energy and twin boundary energy compared with pure metal clusters with fcc structure.

(Received November 28, 2002; Accepted February 19, 2003)

Keywords: *FeN cluster, fcc structure, tetrahedron habit, plasma-gas-condensation*

1. Introduction

Nanoclusters reveal unique physical and chemical properties, which are significantly different from those of their corresponding bulk counterparts.[1–3] Many kinds of metal nanoparticles have been fabricated by various techniques including colloidal chemistry method,[4,5] inert gas condensation,[6–8] laser deposition,[9] mechanical attrition,[10] and electrodeposition.[11] Besides the metal clusters, compound (nitride or oxide) clusters are also interesting because of their excellent oxidation- and corrosion-resistance in comparison with their pure metal clusters. In particular, Fe-nitrides are more attractive because some of them are of excellent magnetic properties, for example, high magnetic flux density of α''-$Fe_{16}N_2$ and γ'-Fe_4N. There have been a few reports on the study of Fe-nitride particles in which γ'-Fe_4N particles were prepared by heating acicular Fe particles in NH_3–H_2 gas mixture[12,13] and by a reactive gas evaporation method in ammonia gas atmosphere.[14,15]

In the present study, an fcc single-phase FeN clusters were obtained by using a combination of reactive sputtering in Ar+N_2 gas atmosphere and gas-condensation cluster deposition technique. Here, we report growth and crystal structure of Fe–N clusters obtained by this method and discuss the origin of a tetrahedral habit of an fcc FeN clusters with a very small size.

2. Experiment

The Fe–N clusters were prepared by the PGC-type cluster beam deposition apparatus, whose detail was described elsewhere.[8,16] The apparatus is composed of the three main parts: a sputtering chamber, a cluster growth room and a deposition chamber. The metal vapors were generated from a Fe target by dc sputtering. A continuous Ar gas stream up to 2.2×10^{-4} mol/s (1 mol/s = 1.34×10^6 sccm, standard cubic centimeter per minute) was injected into the sputtering chamber through a nozzle. A N_2 gas stream up to 3.0×10^{-6} mol/s (4 sccm) was also introduced into the sputtering chamber from a gas inlet. The vaporized atoms in the sputtering chamber are decelerated by collisions with a large amount of Ar gas, and are swept into the cluster growth room, which is cooled by liquid nitrogen. The Fe–N clusters formed by reactive process are ejected from a small nozzle by differential pumping and a part of the cluster beam is intercepted by a skimmer, and then deposited onto a sample holder in the deposition chamber.

The deposition rate of Fe–N clusters was measured by a quartz oscillator-type thickness monitor installed behind the substrate. The microgrid, which was covered by a carbon-coated colodion film and supported by a Cu grid, was used as a substrate for transmission electron microscope (TEM) observation. The size of clusters deposited on the microgrids was estimated by TEM and the crystal structure was analyzed by electron diffraction (ED) patterns. The samples were exposed in air for transportation and observed with the Hitachi HF-2000 TEM operating at 200 kV.

3. Results

Figure 1 shows (a) a typical deposition rate (R_{dep}) of the Fe–N clusters and (b) sputtering current (I) and voltage (V) as a function of N_2 gas flow rate, R_{N_2}, at a constant sputtering power: $P_W = 400$ W. The deposition rate measured by the thickness monitor rapidly decreases with increasing R_{N_2}. Here, it is noted that the sputtering current also decreases rapidly while sputtering voltage increases with increasing R_{N_2}. Hence, the rapid decrease of R_{dep} should mainly result from change of the sputtering condition in the sputtering chamber other than cluster nucleation and growth process in the cluster growth region. Introduction of N_2 gas to the sputtering chamber probably impedes movement of Ar ions toward the Fe target due to collision between Ar ions and N atoms and/or N ion, leading to the decrease of I and R_{dep}.

Figure 2 shows typical bright-field (BF) TEM images of the Fe–N clusters obtained at several R_{N_2}: (a) $R_{N_2} = 0$, (b) 3.7×10^{-7} (0.5 sccm), (c) 7.5×10^{-7} (1 sccm), and (d) 1.1×10^{-6} mol/s (1.5 sccm), respectively. The experimental parameters were as follows: Ar gas flow rate: $R_{Ar} = 2.2 \times 10^{-4}$ mol/s (300 sccm) and $P_W = 400$ W. The

*[1]This Paper was Presented at the Autumn Meeting of the Japan Institute of Metals, held in Suita, on Nov. 3, 2002.

*[2]Corresponding author: pengdl@mse.nitech.ac.jp

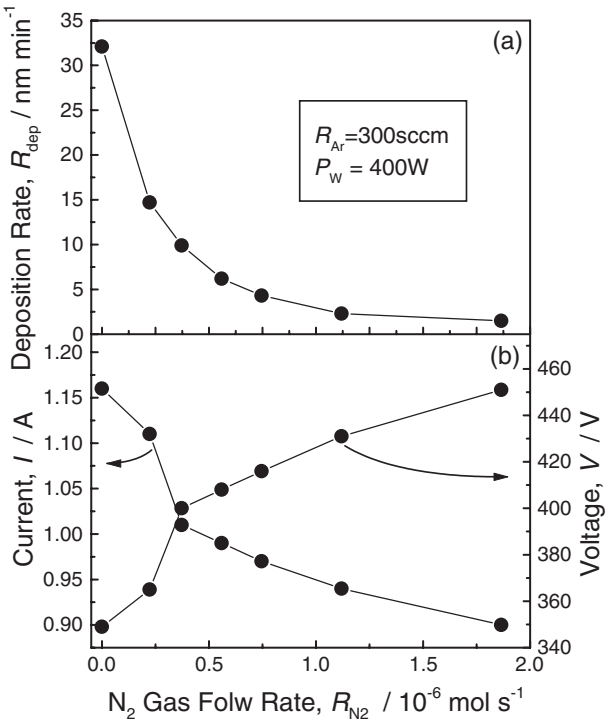

Fig. 1 (a) the deposition rate (R_{dep}) of the Fe–N clusters, and (b) the sputtering current (I) and voltage (V) as a function of N_2 gas flow rate, R_{N_2}, at a constant sputtering power: $P_W = 400$ W.

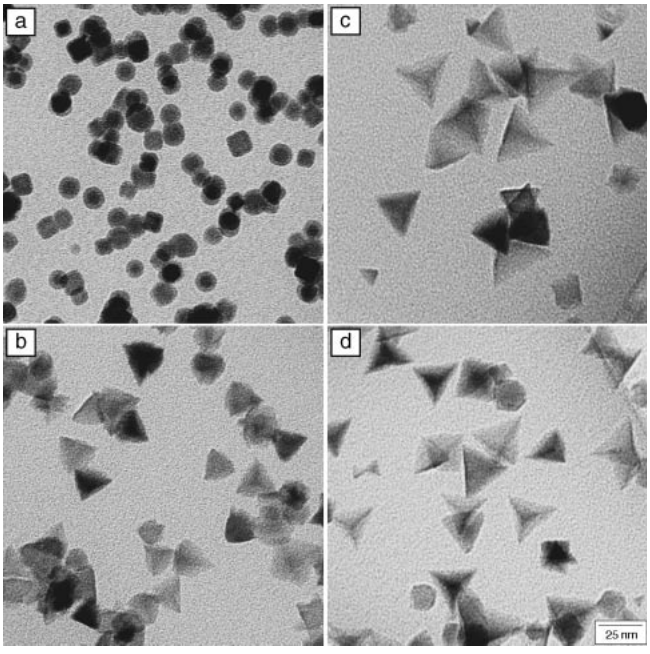

Fig. 2 Bright-field TEM images of the Fe–N clusters obtained at different N_2 gas flow rates, R_{N_2}: (a) $R_{N_2} = 0$, (b) 3.7×10^{-7} (0.5 sccm), (c) 7.5×10^{-7} (1 sccm), and (d) 1.1×10^{-6} mol/s (1.5 sccm).

ED patterns of corresponding heavily stacked cluster assemblies are shown in Figs. 3(a), (b), (c) and (d). At $R_{N_2} = 0$ mol/s, we obtained almost spherical or cubic shape Fe clusters whose mean diameter is about $d = 13$ nm. The ED pattern of these Fe clusters displays one set of diffraction rings of a bcc structure. At $R_{N_2} > 3.7 \times 10^{-7}$ mol/s (0.5 sccm), almost all Fe–N clusters are of a tetrahedron shape with cluster sizes of

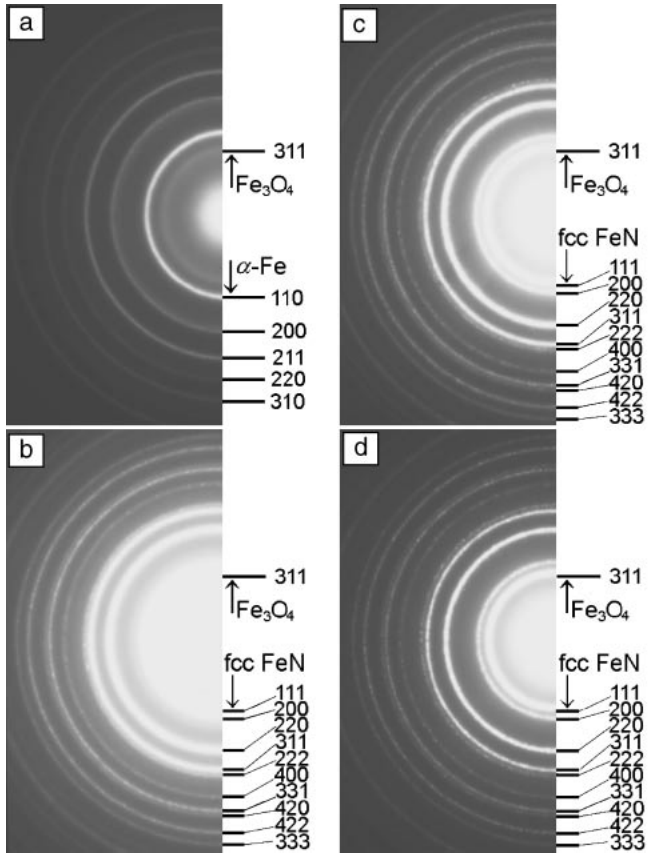

Fig. 3 Electron diffraction patterns of the Fe–N cluster assemblies obtained at different N_2 gas flow rate, R_{N_2}: (a) $R_{N_2} = 0$, (b) 3.7×10^{-7} (0.5 sccm), (c) 7.5×10^{-7} (1 sccm), and (d) 1.1×10^{-6} mol/s (1.5 sccm).

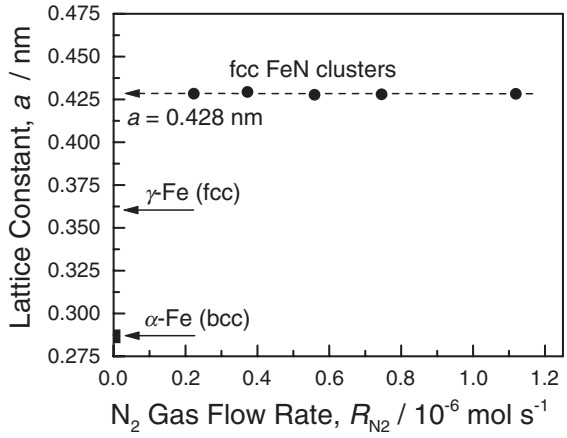

Fig. 4 The estimated lattice constants, a, from the ED patterns for the fcc FeN compound clusters as a function of N_2 gas flow rate, R_{N_2}.

$d = 8$–25 nm. The corresponding ED patterns reveal one set of diffraction rings of an fcc structure. The estimated lattice constants (a) from the ED patterns are shown in Fig. 4. The a value of Fe–N clusters with an fcc structure is independent of R_{N_2}, being about 0.428 nm and close to the experimental value (0.433 nm) of ZnS-type FeN compound films.[17] It is clearly different from that (0.457 nm) of NaCl-type FeN compound films.[18,19]

Figure 5 shows high resolution TEM images of Fe–N clusters obtained at (a) $R_{N_2} = 0$, (b) 3.7×10^{-7} (0.5 sccm),

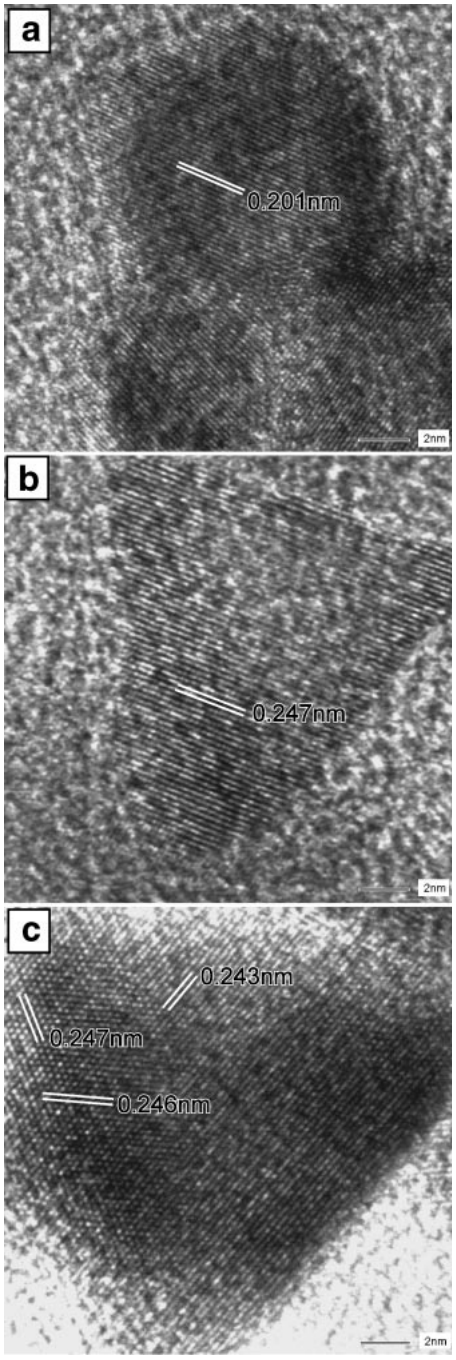

Fig. 5 High resolution TEM images of the Fe–N clusters obtained at (a) $R_{N_2} = 0$, (b) 3.7×10^{-7} (0.5 sccm), and (c) 7.5×10^{-7} mol/s (1 sccm). The lattice fringe ~0.247 nm further suggests the formation of the fcc FeN compound phase.

and (c) 7.5×10^{-7} mol/s (1 sccm), respectively. In Fig. 5(a), the lattice fringe 0.201 nm of pure Fe clusters are easily seen and interpreted to the (110) lattice planes of the bcc structure. For the tetrahedron FeN clusters (Figs. 5(b) and (c)), the (111) lattice planes (with lattice fringe ~0.247 nm) of the fcc structure are easily observed. Moreover, a FeN cluster is viewed along near [111] crystallographic axis and has a threefold symmetry, as shown in Fig. 5(c).

4. Discussion

As shown in the previous section, we have confirmed that the FeN compound clusters with fcc crystal structure are formed in $Ar+N_2$ mixture gas atmosphere. Moreover, almost all FeN clusters have a tetrahedron habit. In general, the minimum energy shape for a given volume is determined by the Wulff construction. This construction gives the equilibrium shape of a free-floating small particle, and is mathematically equivalent to stating that the normal distance from a common center to any given surface facet is proportional to the surface free energy of the facet. However, in many cases (especially for very small particles) the experimental structure is not the Wulff shape, but clearly determined in a large part by growth conditions such as non-free space, a substrate effect, a non-equilibrium state *etc*. A typical example is called multiply-twinned particles (MTPs) for the metals with fcc structure. They are first discovered by Ino,[20,21] and Ino and Ogawa.[22] Ino's original approach to modeling these particles was in terms of arrangements of twin-related tetrahedrons packed along (111) faces. The five units can be arranged to form a pentagonal bipyramid (namely decahedron), and the twenty an icosahedron. From Ino's calculation[20,21] on critical sizes for stable and quasi-stable states of the icosahedral and decahedral particles, an icosahedral particle is essentially stable for $r \leq r_{iw}$ in comparison with an equilibrium Wulff shape, while a decahedral particle is not essentially stable but quasi-stable for $r \leq r_{dt}$, where r is an edge length of the particles, and r_{iw} and r_{dt} are the critical edge lengths. The calculated critical values are in good agreement with experimental results. For single tetrahedral particle, because of its largest total surface area compared with those of the icosahedral and decahedral particles, it becomes quasi-stable only when $r > r_{dt}$. The quasi-stable size $2r_{dt}$ of fcc γ-Fe decahedral particles, for instance, is about 170 nm, being larger by an order of magnitude than the size of the FeN clusters. All FeN clusters reveal a tetrahedron habit, indicating that their sizes are larger than quasi-stable size $2r_{dt}$ of the decahedral particle. As seen in Fig. 2, the size of the FeN tetrahedral clusters is about $d = 8$–25 nm, which is much lower than quasi-stable size $2r_{dt}$ of pure metal with fcc structure.[20,21] This implies that the fcc FeN compound cluster has a very small quasi-stable size $2r_{dt}$.

In order to further discuss the stability of the FeN tetrahedral clusters in such small sizes, we compare total free energies, U_t for a normal tetrahedral particle and U_d for a decahedral multiply-twinned particle. U_t and U_d can be expressed as[20,21]

$$U_t = -U_c + U_s + U_a, \tag{1}$$

$$U_d = -U_c + U_s + U_a + U_{es} + U_{tb}, \tag{2}$$

where U_c, U_s and U_a are the cohesive energy, the surface energy and the adhesive energy to the substrate. Besides them, the elastic strain energy U_{es} and the twin boundary enegy U_{tb} should be added for a multiply-twinned particle. In the present experiment, the fcc FeN clusters have been formed before softly landing onto the substrates in the deposition chamber. Hence, we can consider that the shape of

the cluster is not influenced by the substrates, namely being equivalent to the case of a free space ($U_a = 0$). Assuming that both of these particles contain the same number of atoms or that the volumes are equal to each other, the total free energy difference ΔU_{dt} between the decahedron and tetrahedron can be written as

$$\Delta U_{dt} = U_d - U_t = \left(\frac{5\sqrt{2}}{12} W_d\right) r_d^3 - \left[\frac{\sqrt{3}}{2}(2 \times 5^{2/3} - 5)\gamma_{111} - \frac{5\sqrt{3}}{4}\gamma_t\right] r_d^2 \quad (3)$$

where r_d is an edge length of the decahedron, γ_{111}, γ_t and W_d are the (111) surface energy in unit area, the twin boundary energy in unit area, and the elastic strain energy density, respectively.[20,21] By putting $\Delta U_{dt} = 0$, r_{dt} is easily obtained as

$$r_{dt} = \frac{3\sqrt{6}}{10} \frac{1}{W_d} [2(2 \times 5^{2/3} - 5)\gamma_{111} - 5\gamma_t]. \quad (4)$$

Based upon eq. (4), supposing that the FeN compound has a smaller γ_{111} value and/or larger γ_t and W_d values than those of pure metal Fe, the fcc FeN compound clusters reveal a small r_{dt} value.

5. Conclusion

We have prepared Fe–N clusters by a PGC-type cluster deposition apparatus, and studied their crystal structures by TEM. The fcc single-phase FeN clusters with the lattice parameter $a = 0.428$ nm are obtained. The shape of the FeN clusters depends on the nitrogen gas flow rate R_{N_2}. When $R_{N_2} \geq 7.5 \times 10^{-7}$ mol/s, almost all clusters are of a tetrahedral habit and their sizes are about $d = 8$–25 nm which are smaller by an order of magnitude than the critical size of the pure γ-Fe decahedral particles. This is ascribed to a low (111) surface energy and/or high elastic strain energy and twin boundary energy of the FeN clusters compared with pure metal clusters with fcc structure.

Acknowledgments

One of the authors (D. L. Peng) appreciates the financial support from Japan Society for the Promotion of Science (JSPS).

REFERENCES

1) W. A. de Heer: Rev. Mod. Phys. **65** (1993) 611–676.
2) H. Haberland: *Clusters of Atoms and Molecules I and II*, (Springer-Verlag, Berlin, 1995) pp. 207–252.
3) D. L. Leslie-Pelecky and R. D. Rieke: Chem. Mater. **8** (1996) 1770–1783.
4) C. T. Black, C. B. Murray, R. L. Sandstrom and S. Sun: Science **290** (2000) 1131–1134.
5) S. Sun and C. B. Murray: J. Appl. Phys. **85** (1999) 4325–4330.
6) H. Gleiter: Prog. Mater. Sci. **33** (1989) 223–375.
7) H. Haberland, M. Karrais, M. Mall and Y. Thurner: J. Vac. Sci. Technol. A **10** (1992) 3266–3271.
8) S. Yamamuro, K. Sumiyama, M. Sakurai and K. Suzuki: Supramol. Sci. **5** (1998) 239–245.
9) S. S. Parkin, N. More and K. P. Roche: Phys. Rev. Lett. **64** (1990) 2304–2307.
10) C. C. Koch: Nanostructured Mater. **9** (1997) 13–22.
11) S. Banerjee, S. Roy, J. W. Chen and D. Chakravorty: J. Magn. Magn. Mater. **219** (2000) 45–52.
12) A. Tasaki, K. Tagawa, E. Kita, S. Harada and T. Kusunose: IEEE Trans. Magn. **MAG-17** (1981) 3026–3028.
13) N. Saegusa, A. H. Morrish, A. Tasaki, K. Tagawa and E. Kita: J. Magn. Magn. Mater. **35** (1983) 123–125.
14) K. Yamauchi, S. Yatsuya and K. Mihama: J. Cryst. Growth **46** (1979) 615–619.
15) N. saegusa, T. Tsukagoshi, E. Kita and A. Tasaki: IEEE Trans. Magn. **MAG-19** (1983) 1629–1631.
16) S. Yamamuro, K. Sumiyama and K. Suzuki: J. Appl. Phys. **85** (1999) 483–489.
17) T. Hinomura and S. Nasu: Physica B **237–238** (1997) 557–558.
18) H. Nakagawa, S. Nasu, M. Takahashi and F. Kanamaru: Hyperfine Interact. **69** (1991) 455–458.
19) T. Hara, M. Nishiyama, M. Sato, N. Izumi and S. Nasu: J. Japan Inst. Metals **66** (2002) 929–934.
20) S. Ino: J. Phys. Soc. Jpn. **21** (1966) 346–362.
21) S. Ino: J. Phys. Soc. Jpn. **27** (1969) 941–953.
22) S. Ino and D. Ogawa: J. Phys. Soc. Jpn. **22** (1967) 1365–1374.